Int. J. Heat Mass Transfer. Vol. 36, No. 3, pp. 705–711, 1993
Printed in Great Britain

0017-9310/93 $6.00+0.00
© 1993 Pergamon Press Ltd

Evaporation of polydisperse ethanol aerosols in humid environment

S. V. MANI,† M. KULMALA and T. VESALA
Department of Physics, University of Helsinki, Siltavuorenpenger 20D, SF-00170, Helsinki, Finland

(*Received* 17 *February* 1992)

Abstract—The simultaneous evaporation and condensation of continuum regime ethanol–water droplets have been investigated. The evolution of cumulative mass distribution has been analysed numerically and the model predictions have been compared with the results from wind tunnel experiments. The predictions also include the estimation for the turbulent droplet deposition on the tunnel wall. The strong influence of the relative humidity on the evaporation rate, and furthermore on the mass distribution, is discovered.

INTRODUCTION

EVAPORATION and condensational growth of droplets are fundamental processes in the atmosphere and also in many industrial operations employing liquid sprays and liquid fuel combustion. Further, most of the atmospheric and industrial aerosols are often polydisperse, that is they contain a wide range of droplet/particle sizes and hence the study of the evaporation behaviour of polydisperse aerosols is of great practical importance.

Although experimental and theoretical investigations on the evaporation and condensational growth of single droplets have been well established and reviewed by Davies [1], Wagner [2] and Davis [3], experimental measurements on polydisperse aerosols are almost non-existent, while few theoretical studies have been reported by Probert [4], Dickinson and Marshall [5] and Tsang *et al.* [6].

The evaporation/gasification of volatile aerosols such as methanol and ethanol in humid environment has been the subject of considerable interest due to the fact that the large heat release due to the condensation of ambient water vapour on evaporating volatile droplets substantially augments the evaporation process as was first suggested by Law and Binark [7]. This concept was later substantiated experimentally and theoretically by Law *et al.* [8] for single methanol and ethanol droplets.

We present experimental and numerical results for polydisperse ethanol aerosols (10–200 μm) evaporating in humid air. The main stress is laid on the description of processes governing the evolution of the cumulative mass distribution and on the interpretation of obtained results.

EXPERIMENTAL

The experimental investigation of the evaporation of polydisperse ethanol aerosols in a vertical wind tunnel involved the measurement of changes in droplet size distribution with downstream distance from the inlet. A schematic diagram of the wind tunnel and the associated equipment is shown in Fig. 1 [9].

Air was drawn from the atmosphere by a blower (1) of 1000 $m^3\ h^{-1}$ capacity, through a calibrated orifice meter (2) and an absolute HEPA filter (4) before entering the 5 m long and 0.15 m diameter main wind tunnel section. The wind tunnel was constructed of circular cross-sectioned hard PVC pipe. The flow velocity in the wind tunnel was typically 4–5 $m\ s^{-1}$, which gives for the pipe a Reynolds number of about 37 000–46 000. Ethanol aerosol was generated by pumping pure ethanol from a storage tank (7) by a centrifugal pump (3) through a pressure atomising nozzle (9) capable of generating droplets in the diameter range of 10–200 μm. Ethanol flow rate and atomizing pressure were measured by a calibrated rotameter (5) and pressure gauge (6), respectively. The liquid deposited on the wind tunnel wall was collected by a small concentric slot at the bottom of the wind tunnel.

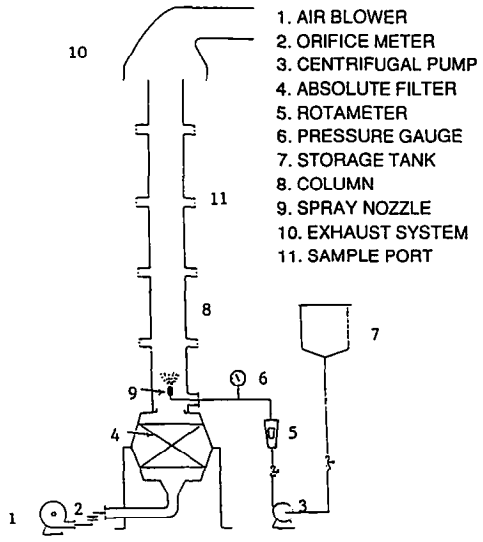

FIG. 1. Schematic diagram of experimental equipment [9].

† Visiting Scientist in University of Helsinki.

NOMENCLATURE

a	droplet radius
Ci	correction factor for diffusion coefficient
d	droplet diameter
d'	size parameter indicating the peak in the distribution
D_{il}	binary diffusion coefficient of species i
D_c	diameter of pipe
erfc	complementary error function
I_i	gas-phase mass flux vapour i
K	thermal conductivity of the gas mixture above the droplet
L_i	latent heat of vaporization for species i
L	length of pipe
M_i	molecular weight of species i
m	total droplet mass
m_i	liquid mass of species i
n	width parameter in Rosin–Rammler distribution
p	total pressure
P	fractional penetration of droplets in pipe
p_i	partial vapour pressure above the droplet surface
Q	gas-phase heat flux
Q_g	volumetric flow rate of fluid through the pipe
R	gas constant
T	temperature
u^*	friction velocity
V	deposition velocity
v_f	volume or mass fraction of spray
V_+	dimensionless deposition velocity
X_i	mole fraction of species i in the droplet.

Greek symbols

α_+	inverse of dimensionless relaxation time
β_{Mi}	transitional correction factor for mass transfer
β_T	transitional correction factor for heat transfer
η	ratio of dimensionless r.m.s. droplet velocity to dimensionless r.m.s. fluid velocity
μ_g	viscosity of gas
ρ_d	density of droplet
ρ_g	density of gas
τ_+	dimensionless droplet relaxation time.

Subscripts

a	values at droplet surface
i	species
1	species
2	species
∞	values far from the droplet.

The main section of the wind tunnel was equipped with four sample ports each separated by a distance of 1 m. Each sample port was covered by a 0.04 m diameter flat glass window to allow passage of the laser beam through the pipe cross-section. The ethanol droplets generated by the nozzle were allowed to attain the gas velocity and to disperse evenly in the 1.25 m pipe section between the nozzle and the first sample port.

A Malvern Laser Droplet Detector (Malvern Instruments Ltd, U.K.) was used for the *in-situ* measurements of droplet size distributions along the tunnel. The instrument was oriented at various sample ports by means of a winch and pulley arrangement shown in Fig. 2 [9]. This consisted of a metallic v-bracket (not shown in the figure) which moved up and down a metallic beam (4) aligned parallel to the pipe and fixed to the floor. The winch (1) was designed to lift 500 kg and hence the laser instrument could be safely aligned across the tunnel to measure droplet size distribution at various sample ports downstream without disturbing the flow pattern of the gas stream.

The temperature and relative humidity of the incoming air through the wind tunnel were also measured before sample port 1. The ambient temperature was measured by a thermometer inserted in the air line before the absolute filter. The relative humidity of the air was estimated by measuring the dew point by a condensation type dew point hygrometer (EG & G model 800) and then converting it to absolute humidity and hence the vapour content of the air flowing.

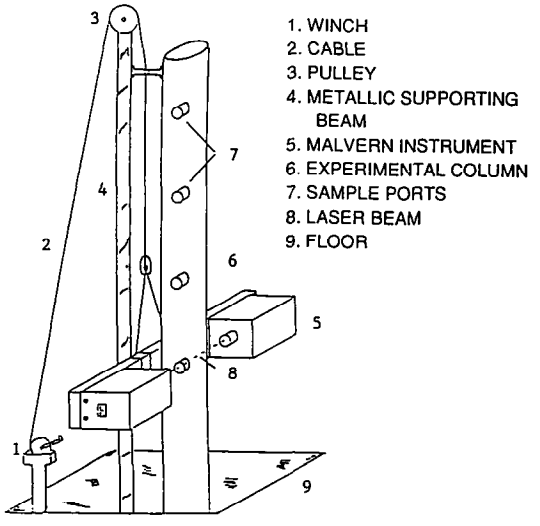

FIG. 2. Schematic diagram of the orientation of the Malvern instrument [9].

The procedure for an experimental run is as follows: After preparing the experimental system, initially air was drawn from the atmosphere through the column at the desired flow rate until a steady temperature was attained and then the dew point was measured. Meanwhile, pure ethanol in the storage tank was continuously circulated through the pump to bring it to the air temperature in the tunnel. Then the laser instrument was oriented at sample port 1 and a blank reading of the air flow was taken before injecting ethanol spray. After a steady state had been achieved, the size distribution of the aerosol was obtained. Then the instrument was taken to sample port 2 by means of the winch and pulley arrangement and the same procedure was repeated to obtain size distribution at sample port 2. At each sample port a fresh bank measurement was made before obtaining the actual distribution of the aerosol. During the experimental runs it was found that the ethanol droplet concentration fell below the minimum concentration required by the Malvern instrument, beyond sample port 2 and hence further measurements could not be made at sample ports 3 and 4. This was due to the fast evaporation of ethanol droplets.

The built-in software associated with the instrument enabled a Rosin–Rammler distribution to be taken at each sample port with the parameters of the distribution d' and n determined. The Rosin–Rammler distribution is usually expressed in terms of cumulative undersize weight as

$$v_f = 1-\exp\left(-\left(\frac{d}{d'}\right)^n\right) \quad (1)$$

where v_f represents the volume or mass fraction of spray less than the diameter d, d' a size parameter approximately indicating the position of the peak of the weight frequency distribution and n a distribution width parameter with narrrow distributions giving high n values and vice versa. The Rosin–Rammler distribution has been widely applied for modelling the distribution of droplet sizes generated by various atomizing nozzles [10].

THEORETICAL

The theoretical model used to predict the change in droplet size distribution with position along the wind tunnel involves the calculation of the change in diameter of each droplet comprising the aerosol due to evaporation, condensation and turbulent deposition. It has been assumed that the relative velocity between gas and droplets in the axial direction is negligible, since the gas is travelling many times faster than the terminal velocity of the largest drop considered in this study. Similarly, re-entrainment of droplets from the wind tunnel walls has been assumed to be absent, since the droplets deposited on the walls were observed to coalesce rapidly into a thin film and hence any re-entrainment would be as vapour and not droplets.

Evaporation of droplets

Droplet evaporation or condensation rate depends on the net transport of vapour molecules relative to the droplet. The mass transfer is accompanied by heat transfer, because at the phase transitions heat is released (condensation) or consumed (evaporation). Since the vapour diffusion and heat conduction in the gas proceed on a much faster time scale than evaporation or condensation, the vapour concentrations and the temperature profiles near the droplet approach steady state before appreciable evaporation or condensation occurs and the mass and heat fluxes can be considered as quasi-steady [11]. Changes in these processes are determined by the changing boundary conditions, i.e. by changing surface mole fractions and surface temperature. Furthermore, the mole fractions and the droplet temperature are spatially uniform within the droplet but temporally varying.

The quasi-steady evaporation or growth rate for a binary droplet can be written as

$$\frac{dm_1}{dt} = I_1(m, X_1, T_a) \quad \frac{dm_2}{dt} = I_2(m, X_2, T_a) \quad (2)$$

where m_i represents the liquid mass of species i and I_i the gas-phase mass flux of the vapour i. m is the total droplet mass ($m = m_1 + m_2$) and X_i the mole fraction of species i in the droplet, T_a is the droplet temperature.

In the continuum regime, the expressions for mass fluxes due to ordinary diffusion result from the Stefan–Maxwell equations and they are coupled in a quite complex manner [12]. However, the assumption of independent, uncoupled diffusion is entitled to be used for conditions considered in this study (see ref. [13]) and the simplified mass flux expressions are given by [14]

$$I_1 = -\frac{4\pi a M_1 D_{1l,\infty} p \beta_{M1}}{RT_\infty} C_1 \ln\left(\frac{1-p_{1\infty}/p}{1-p_{1a}/p}\right)$$

$$I_2 = -\frac{4\pi a M_2 D_{2l,\infty} p \beta_{M2}}{RT_\infty} C_2 \ln\left(\frac{1-p_{2\infty}/p}{1-p_{2a}/p}\right) \quad (3)$$

where R is the gas constant, M_i the molecular weight of species i and p the total pressure. $D_{il,\infty}$ is the binary diffusion coefficient of species i with respect to an inert gas at the temperature far from the droplet, T_∞. a is the droplet radius, which is determined by the total mass of the droplet and the overall droplet density as usual. p_{ia} and $p_{i\infty}$ are the partial vapour pressures just above the droplet surface and far from it, respectively. In calculating p_{ia}, the droplet surface can be assumed to be saturated. The disturbance of the saturation equilibrium is taken into account by the transitional correction factor $\beta_{M,i}$, which is a function of the Knudsen number for mass transfer and the mass accommodation coefficient for each species [2, 15]. The correction factor C_i, which takes into account the

temperature dependence of the diffusion coefficient $D_{il}(T) = D_{il,\infty}(T/T_\infty)^{\mu_i}$, is [14]

$$C_i = \frac{T_\infty - T_a}{T_\infty^{\mu_i - 1}} \frac{2-\mu_i}{T_\infty^{2-\mu_i} - T_a^{2-\mu_i}}. \quad (4)$$

In the above expressions, the mass transfer rates of vapours are governed by ordinary diffusion (and convective-like Stefan flow) in the pure inert gas, neglecting another vapour. The effect of another vapour is introduced only by the boundary conditions at the droplet surface.

An equation for the steady state droplet temperature can be derived using the energy conservation. Neglecting the droplet heat capacity, the temperature levels off at a value where the phase transition heats can be transferred in the gas; i.e.

$$Q(a, T_a) + L_1 I_1 + L_2 I_2 = 0 \quad (5)$$

where Q is the gas-phase heat flux (excluding the contribution from the enthalpies of diffusing vapours) and L_i is the latent heat of vaporization for species i including liquid mixing enthalpy.

If the heat flux is governed merely by thermal conduction according to Fourier's law and if the thermal conductivity is allowed to vary linearly with temperature, the droplet temperature can be expressed as [2, 14]

$$T_a = T_\infty + \frac{L_1 I_1 + L_2 I_2}{2\alpha a (K_\infty + K_a)\beta_T} \quad (6)$$

where K_a and K_∞ are the thermal conductivities of the gas mixture just above the droplet surface and far from it, respectively. The transitional correction factor β_T is a function of the Knudsen number for heat transfer and the thermal accommodation coefficient [2, 16].

Deposition

In addition to droplet evaporation and condensation the theoretical model accounts for the deposition of droplets onto the wind tunnel wall.

Particle or droplet deposition in turbulent flow can occur by gravitational, inertial and electrostatic forces or by Brownian motion. Friedlander and Johnstone [17] have shown that for electrically neutral aerosols larger than 1 μm in diameter, the predominant deposition mechanism in vertical pipes is inertia.

In the present analysis, we have applied the stochastic model of Reeks and Skyrme [18], proposed to explain the experimental results obtained by Liu and Agarwal [19], who presented their data in the Reynolds number range 10 000–50 000, as a universal curve of τ_+ (the dimensionless droplet relaxation time) vs V_+ (the dimensionless deposition velocity). The data were fitted into the stochastic model by adjusting the constants in the following expression for deposition velocity

$$V_+ = 0.56\eta \operatorname{erfc}\left(\frac{6.25\alpha_+}{\sqrt{2\eta}}\right)$$

$$\alpha_+ = 1/\tau_+$$

$$\tau_+ = \frac{d^2 \rho_g \rho_d u^{*2}}{18\mu_g^2} \quad (7)$$

where u^* is the friction velocity which is related to the average velocity of the fluid in the pipe through the pipe friction factor and $V_+ = V/u^*$ [18]; η the ratio of r.m.s. droplet velocity to r.m.s. fluid velocity estimated according to ref. [18]; and erfc the complementary error function, ρ_d and ρ_g the densities of droplet and gas, respectively, and μ_g the viscosity of the gas.

Equation (7) can be used to calculate V_+ for a droplet of given τ_+ and hence the deposition velocity V can be obtained. Once the deposition velocity V has been evaluated, it is necessary to calculate the fractional penetration of droplets, P, and hence the fractional deposition of droplets on the wall, $(1-P)$. The fractional penetration can be calculated from (e.g. ref. [20])

$$V = \frac{Q_g}{\pi D_c L} \ln(1/P) \quad (8)$$

where Q_g is the volumetric flow rate of fluid through the pipe, D_c the pipe diameter, L the pipe length.

The foregoing analysis breaks down for τ_+ less than 5. In our experimental conditions, for τ_+ below 5, the empirical relation of Liu and Agarwal [19] given by

$$V_+ = 6.0 \times 10^{-4} \tau_+^2 \quad (9)$$

has been used.

Numerical

The numerical model includes detailed submodels for quasistationary evaporation and condensation processes and for turbulent droplet deposition. Equations (2) and (3) are solved by means of fourth-order Runge–Kutta method [21] and the droplet temperature (equation (6)) is solved using the Newton–Raphson method [21]. A detailed description of the condensation/evaporation part of the numerical model is presented by Majerowicz *et al.* [22]. Turbulent deposition is estimated according to ref. [19]. A detailed description of the deposition part is presented by Mani [9].

The overall aerosol dynamical model is simplified. We treat the depositing polydisperse droplets as a system comprising several (200 in our calculations) separate monodisperse populations with different droplet sizes. This approach is legitimate, since droplet mass concentrations are fairly low (see the next section and Table 1).

To calculate evaporation/condensation and deposition the physico-chemical data about water–ethanol mixture are needed. The model computations require values of various physico-chemical properties which may be constant or may depend on the temperature

and the composition. The correlations of experimental values for these properties are found in the literature. Molecular weights, binary diffusion coefficients, thermal conductivities, dynamic viscosities, saturation vapour pressures and liquid and vapour specific enthalpies (including latent heats of vaporization) are estimated according to refs. [23–27]. The thermal conductivity of gaseous mixtures is calculated from the pure component conductivities by an equation developed by Lindsay and Bromley [28]. The activity coefficients were determined from three parameter Redlich–Kister equation of d'Avila and Silva [29]. The density fit based on the data of Perry and Chilton [30] was used. The saturation vapour pressure of the pure ethanol was taken from ref. [31].

RESULTS AND DISCUSSION

We consider the evaporation behaviour of the ethanol droplet population in humid air. The effects of the droplet mass concentration and deposition are examined numerically. Finally, the overall behaviour of the droplet population is analysed and the numerical results are verified by an example of experimental results.

Table 1 shows the sensitivity of the final diameter of an ethanol droplet to the presence of water vapour and to the total droplet mass concentration. The final diameter corresponds to the diameter after 0.20 s. The gas temperature is 33°C and in the presence of water vapour the relative humidity is 66%.

Firstly, consider the effect of the water vapour condensation on the final diameter. The condensation of water vapour has two opposing simultaneous effects on the droplet size. The condensed water naturally tends to increase directly the droplet size; on the other hand the latent heat released in condensation tends to raise the droplet temperature and therefore enhances evaporation and furthermore tends to decrease the droplet size (see also refs. [8, 32]). The significance of these effects depends on the initial droplet size. For smaller droplets the direct effect of condensed water is important whereas for larger droplets the effect resulting from the latent heat becomes more significant. The droplets of initial diameter of up to 30 μm evaporate completely in the dry air, while the droplets of above 10 μm in diameter remain in the aerosol (as almost pure water droplets) in the presence of water vapour. For droplets of above 50 μm, there is relatively less time to evaporate during 0.2 s as for smaller droplets and water vapour condensation decreases the final diameter by means of enhanced evaporation.

Table 1. Effect of water vapour condensation on ethanol droplets and effect of droplet mass concentration. The final diameter corresponds to the diameter after 0.20 s. The gas temperature is 33°C and in the presence of water vapour the relative humidity is 66%. ID, initial drop diameter (μm); FD, final diameter (μm); A, condensation absent; B, condensation present, single droplet; C, condensation present, total initial mass concentrations of droplets 0.8 g m^{-3}; D, condensation present, total initial mass concentration of droplets 8 g m^{-3}

ID	A FD	B FD	C FD	D FD
10	0.00	0.00	0.00	0.00
20	0.00	7.71	7.87	9.10
30	0.00	15.98	16.07	16.80
40	16.30	23.04	23.11	23.72
50	34.16	30.18	30.29	31.38
60	47.46	40.72	40.88	42.52
70	59.60	52.73	52.89	54.32
80	71.08	64.41	64.54	65.78
90	82.18	75.72	75.84	76.92

Secondly, consider the effect of the mutual droplet interactions through changes in ambient conditions. As evaporation (condensation) proceeds, the vapour pressure in the gas increases (decreases) and the gas temperature decreases (increases). When the droplet mass concentration increases, the effect of the mutual interactions becomes naturally more pronounced. The mutual interactions have slight effect when the total mass concentration is below 0.8 g m^{-3}. In this investigation the concentration is below that value and hence we can treat the depositing polydisperse droplets as a system comprising several separate monodisperse populations with different droplet sizes, i.e. the overall effect of the deposition on the ambient conditions can be legitimately neglected. Note also that the number concentration of particles is low enough so that droplet coagulation can be neglected.

We have investigated theoretically the evolution of ethanol droplet population in the presence of deposition with different relative humidities. Firstly, we compare the relative effects of evaporation/condensation and deposition on droplet mass changes. The cumulative mass distribution of initially pure ethanol droplets has been set to increase linearly with increasing droplet diameter. Table 2 presents the changes in droplet masses resulting from deposition and evaporation/condensation after 0.2 s for relative humidities 0, 60 and 90%. The gas temperature is 30°C. The effect of deposition on mass changes is significantly smaller than evaporation/condensation processes in all size classes. The overall mass change by deposition is about 7% and by evaporation/condensation over 60% for all relative humidities. The total change is about 70% in these conditions.

Figure 3 shows the evolution of the cumulative mass distribution for the cases described just above. The distribution alters most with the relative humidity 0%. The change is mainly caused by evaporation as noted above. Small droplets evaporate relatively more than larger droplets during 0.2 s, since the evaporation is governed by the well-known a^2-law (resulting if the mass flux is expressed by means of the droplet density and the evaporation rate da/dt, and equalized with expression (3)). Thus the distribution evolves from the initially linear form to such a form that lies below the initial curve for smaller diameters and intersects

Table 2. Effects of deposition and evaporation/condensation on the droplet masses as a function of the initial droplet diameter (ID) in μm with different relative humidities. The gas temperature is 30°C and the flow velocity is 4.0 m s^{-1}. The numbers describe the percentage change in the droplet mass after 0.2 s caused by deposition (DEP) or evaporation/condensation (EVA/CON) processes (e.g. 100 in column EVA/CON means that droplets in the size class concerned have disappeared completely by evaporation)

	RH = 0%		RH = 60%		RH = 90%	
ID	DEP	EVA/CON	DEP	EVA/CON	DEP	EVA/CON
10	0	100	0	100	0	95
20	0	100	0	97	0	80
30	0	100	1	86	1	76
40	7	89	7	77	6	71
50	16	61	16	65	18	61
60	14	46	14	57	15	60
70	11	37	11	49	12	54
80	9	30	10	40	10	46
90	7	25	8	35	8	40
100	6	21	7	30	7	35

it at the larger end of the distribution. At higher relative humidities the distribution evolves similarly, but the change is reduced substantially for smaller droplets. This results naturally from the contribution of the condensed water to the droplet masses (see Table 1). However, for larger droplets at higher relative humidities, the change (compared with the initial distribution) is enhanced since the evaporation rate is increased due to latent heat released in water condensation (see Table 1).

The behaviour of the ethanol droplet population in the humid air is also investigated experimentally. A comparison between experimental [9] and theoretical results for cumulative mass distribution fitted to equation (1) is shown in Fig. 4. The relative humidity is 62%, the gas temperature is 34°C and the flow velocity is 4.0 m s^{-1}. The final distribution has evolved from the initial one during 0.25 s. The parameters d' and n (see equation (1)) for the initial distribution is 58.35 μm and 1.20, for the experimental final distribution 72.42 μm and 2.13, and for the theoretical final distribution 84.42 μm and 2.01, respectively. The agreement between results is fairly good and the evolution of the distribution resembles the behaviour presented in Fig. 3. If the effect of the condensing water vapour was neglected (RH = 0%), the discrepancy between experimental and theoretical results would become much larger (see also ref. [33]). With higher relative humidities (about 80%) experimental distributions behave qualitatively according to Fig. 3 and the discrepancy between experimental and theoretical distributions is fairly small (see also ref. [9]).

CONCLUSIONS

The evaporation of polydisperse ethanol droplets in a humid environment has been studied. It has been shown that a simplified aerosol dynamical model with detailed submodels of ethanol evaporation, water condensation and of turbulent droplet deposition is able to explain the experimental results obtained in

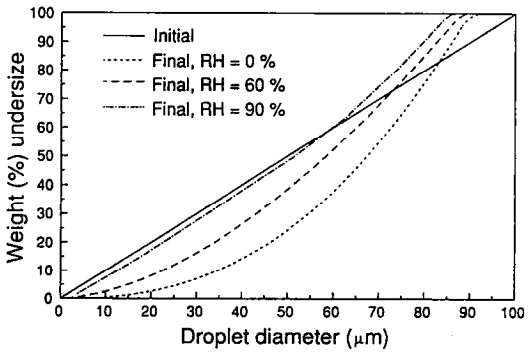

FIG. 3. Evolution of initially linearly increasing cumulative mass distribution for different relative humidities. The final distributions correspond to the distributions after 0.20 s. The gas temperature is 30°C and the flow velocity is 4.0 m s^{-1}.

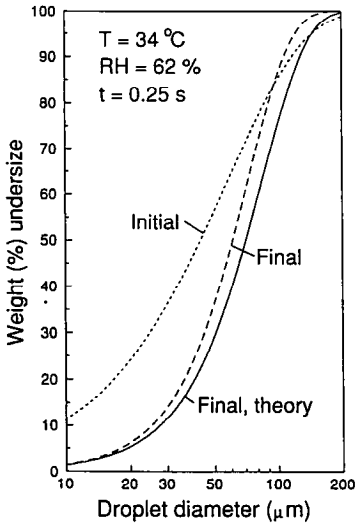

FIG. 4. Evolution of cumulative mass distribution obtained from experiments [9] and by numerical model. The flow velocity is 4.0 m s^{-1}.

earlier studies. The results reconfirm the studies of Dickinson and Marshall [5], Law *et al.* [8] and Tsang *et al.* [6]. Whilst evaporation tends to eliminate completely smaller droplets, the effect of condensation is to increase the proportion of smaller droplets and reduce the droplet mass at the larger end of the cumulative mass distribution. The influence of deposition on the cumulative mass distribution is marginal.

Acknowledgements—S. V. Mani would like to thank the Australian Research Council and University of Newcastle for the financial support for carrying on the experimental investigation. The financial support of the Academy of Finland is also acknowledged.

REFERENCES

1. C. N. Davies, Evaporation of airborne droplets. In *Fundamentals of Aerosol Science*. Wiley, New York (1978).
2. P. E. Wagner, Aerosol growth by condensation. In *Aerosol Microphysics II*, pp. 129–178. Springer, Berlin (1982).
3. E. J. Davis, Transport phenomena with single aerosol particles, *Aerosol Sci. Technol.* **2,** 121–141 (1983).
4. R. P. Probert, The influence of spray particle size and distribution of oil droplets, *Phil. Mag.* **37,** 94–105 (1946).
5. D. R. Dickinson and W. R. Marshall, Jr., The rates of evaporation of spray, *A.I.Ch.E. Jl* **14,** 541–552 (1968).
6. T. H. Tsang, S. M. Cook and M. E. Marra, Dynamic behaviour of condensation and evaporation of polydisperse volatile aerosols, *Aerosol Sci. Technol.* **12,** 386–398 (1990).
7. C. K. Law and M. Binark, Fuel spray vaporization in humid environment, *Int. J. Heat Mass Transfer* **22,** 1009–1020 (1979).
8. C. K. Law, T. Y. Xiong and C. H. Wang, Alcohol droplet vaporization in humid air, *Int. J. Heat Mass Transfer* **30,** 1435–1443 (1987).
9. S. V. Mani, Evaporation of polydisperse aerosols at ambient conditions, Ph.D. Thesis, University of Newcastle, Australia (1988).
10. B. J. Azzopardi, G. Freeman and P. B. Whalley, Drop sizes in annular two phase flow, Report AERE-R9674, UKAEA, England (1978).
11. J. H. Seinfeld, *Atmospheric Chemistry and Physics of Air Pollution*. Wiley, New York (1986).
12. J. Kalkkinen, T. Vesala and M. Kulmala, Binary droplet evaporation in the presence of an inert gas: an exact solution of the Maxwell–Stefan equations, *Int. Commun. Heat Mass Transfer* **18,** 117–126 (1991).
13. T. Vesala, Binary droplet evaporation and condensation as phenomenological processes, Ph.D. Thesis, Department of Physics, University of Helsinki, *Commentationes Physico-Mathematicae et Chemico-Medicae*, Vol. 127. The Finnish Society of Sciences and Letters, Helsinki (1991).
14. M. Kulmala and T. Vesala, Condensation in the continuum regime, *J. Aerosol Sci.* **22,** 337–346 (1991).
15. N. A. Fuchs and A. G. Sutugin, *Highly Dispersed Aerosols*. Ann Arbor Science, Ann Arbor, Michigan (1970).
16. V. I. Smirnov, The rate of quasi-steady growth and evaporation of small drops in a gaseous medium, *Pure Appl. Geophys.* **86,** 184–194 (1971).
17. S. K. Friedlander and H. F. Johnstone, Deposition of suspension particles from turbulent gas stream, *Ind. Engng Chem.* **49,** 1151–1156 (1957).
18. M. W. Reeks and G. Skyrme, The dependence of particle deposition velocity on particle inertia in turbulent pipe flow, *J. Aerosol Sci.* **1,** 485–495 (1976).
19. B. Y. H. Liu and J. K. Agarwal, Experimental observation of aerosol deposition in turbulent flow, *J. Aerosol Sci.* **5,** 145–155 (1974).
20. G. A. Sehmel, Aerosol deposition from turbulent air streams in vertical conduits, Pacific Northwest Lab. Rep. BNWL-578, Richland, Washington (1968).
21. W. H. Press, B. P. Flannery, S. A. Teukolsky and W. T. Vetterling, *Numerical Recipes*. Cambridge University Press, New York (1986).
22. A. Majerowicz, M. Kulmala and P. E. Wagner, Intercomparison of various computational methods for calculation of condensation growth. In *Report Series in Aerosol Science*, Vol. 17, pp. 144–151. Finnish Association for Aerosol Research, University of Helsinki, Helsinki (1991).
23. Landoldt-Bornstein, *Zahlenwerte und Functionen aus Physik-Chemie-Astronomie-Geophysik-Technik*. Springer, Berlin (1960).
24. J. Timmermans, *The Physico-chemical Constants of Binary Systems*, Vol. 4. Interscience, New York (1965).
25. *CRC Handbook of Chemistry and Physics* (66th Edn). The Chemical Rubber Co., Cleveland, Ohio (1985).
26. G. W. C. Kaye and T. H. Laby, *Tables of Physical and Chemical Constants*. Longman, New York (1986).
27. R. C. Reid, J. M. Prausnitz and B. E. Poling, *The Properties of Gases and Liquids* (4th Edn). McGraw-Hill, New York (1987).
28. A. L. Lindsay and L. A. Bromley, Thermal conductivity of gas mixtures, *Ind. Engng Chem.* **42,** 1508–1511 (1950).
29. S. G. d'Avila and R. S. F. Silva, Isothermal vapour–liquid equilibrium data by total pressure method, systems acetaldehyde–ethanol, acetaldehyde–water and ethanol–water, *J. Chem. Engng* **15,** 421–424 (1970).
30. R. H. Perry and C. H. Chilton, *Chemical Engineers' Handbook*. McGraw-Hill, New York (1973).
31. T. Schmeling and R. Strey, Equilibrium vapour pressure measurements for the *n*-alcohols in the temperature range from −30°C to +30°C, *Ber. Bunsenges* **87,** 871–874 (1983).
32. T. Vesala and J. Kukkonen, A model for binary droplet evaporation and condensation, and its application for ammonia droplets in humid air, *Atmos. Environ.* **26A,** 1573–1581 (1992).
33. S. V. Mani, T. Vesala, J. A. Raper and G. J. Jameson, Evaporation of polydisperse organic aerosols at ambient conditions, *J. Aerosol Sci.* **22,** Suppl. 1, S81–S84 (1991).